


Article

Nonlinear Tunability of Elastic Waves in One-Dimensional Mass-Spring Lattices Attached with Local Resonators

Nansun Shen, Jinhui Jiang ^{*}, Fang Zhang ^{*}  and Ming Ding

State Key Laboratory of Mechanical Structure, Mechanics and Control,
Nanjing University of Aeronautics and Astronautics, Nanjing 210016, China
^{*} Correspondence: jiangjinhui@nuaa.edu.cn (J.J.); zhangfangyy@163.com (F.Z.)

Abstract: Vibration propagates in the form of elastic waves. The tuning of elastic waves is of great significance for vibration and noise reduction. The elastic metamaterials (EMs), which can effectively prohibit elastic wave propagation in the band gap frequency range, have been widely studied. However, once the structures of the EMs are determined, the band gap is also determined. In this paper, a discrete nonlinear elastic metamaterial is proposed. The harmonic balance method is used to derive the nonlinear dispersion relation combined with Bloch's theorem. The low frequency band gap near the linear natural frequency of local resonators is obtained. The theoretical results show that the nonlinearity will change the starting and ending frequencies of the band gap. In addition, amplitude can also influence the band gap. This means that the amplitude can be changed to achieve the tunability of elastic waves in nonlinear elastic metamaterials. Finally, the theoretical results are verified by numerical simulation, and the results are in good agreement with each other.

Keywords: elastic waves; nonlinearity; elastic metamaterial; band gap; harmonic balance method; Bloch's theorem



Citation: Shen, N.; Jiang, J.; Zhang, F.; Ding, M. Nonlinear Tunability of Elastic Waves in One-Dimensional Mass-Spring Lattices Attached with Local Resonators. *Aerospace* **2022**, *9*, 818. <https://doi.org/10.3390/aerospace9120818>

Academic Editor: Rosario Pecora

Received: 19 November 2022

Accepted: 10 December 2022

Published: 12 December 2022

Publisher's Note: MDPI stays neutral with regard to jurisdictional claims in published maps and institutional affiliations.



Copyright: © 2022 by the authors. Licensee MDPI, Basel, Switzerland. This article is an open access article distributed under the terms and conditions of the Creative Commons Attribution (CC BY) license (<https://creativecommons.org/licenses/by/4.0/>).

1. Introduction

In the aerospace field, from unmanned aerial vehicles (UAVs) to manned aircrafts, vibration not only affects the confidentiality of instruments and the comfort of passengers, but also causes hidden dangers for flight safety. Vibration and noise also widely exist in various fields such as mechanical engineering, vehicle engineering and so on. Reducing harmful vibration has always been an urgent problem to be solved in engineering technology [1–3]. Phononic crystals (PCs) and elastic metamaterials provide a new way to solve this problem. PCs and EMs are artificially designed periodic structures [4–14]. They possess band gaps (BGs) in which elastic waves are prohibited, while they can propagate in other frequency regions without exhaustion. This makes it possible to achieve wave guiding [15], acoustic filter [16], acoustic cloaking [17], vibration control [18,19], noise reduction [20], acoustic focusing [21,22], non-destructive testing [23], etc. Compared with PCs, EMs can produce band gaps caused by local resonance at lower frequencies.

However, the BGs of EMs are usually fixed once the structures have been designed and fabricated. On the contrary, it is desirable to tune the BGs dynamically or adaptively in most practical applications after they have been fabricated. In recent years, some methods have been proposed to overcome this limitation, such as initial stresses [24,25], piezoelectric materials [26,27], temperature variation [28], external mechanical loads [29] and the space-time modulation elastic metamaterials [30].

Scholars mainly adjust the band gap structure of linear EMs by adjusting their geometric structure and composition. However, in many engineering applications, structures undergo large deformations, such that linear analysis would no longer apply. Nonlinear elastic metamaterials (NEMs) have attracted significant attention recently. Some interesting wave propagation phenomena have been shown in NEMs, such as amplitude-dependent

band gaps [31–33], bifurcations [34] and chaotic bands [35,36]. These make it possible to tune the BGs by nonlinear tunability. Vakakis and King used standing wave solutions to study the amplitude-dependent attenuation zone of a one-dimensional periodic chain with cubic nonlinearity [37]. Cang He [13] used the string to shift the Bragg and local resonance band gaps. The tension produced by the string is cubic nonlinear. Silva et al. [38] showed that the tunable band gap depended on the amplitude through the metamaterial with the quadratic nonlinear resonators.

In this paper, we proposed a nonlinear elastic metamaterial made of linear mass-spring chains with nonlinear oscillators attached to the masses. Many methods have been developed to study the nonlinear band gap, including multiple timescale approaches [39], perturbation methods [12] and incremental harmonic balance methods [40]. Compared with other methods, the harmonic balance method is suitable for a strong nonlinear system and its solving process is more concise. Hence, we apply the harmonic balance method to calculate the dispersion relation of the proposed structure. A concise amplitude-dependent dispersion relation is obtained. The results show that the mass ratio, linear stiffness ratio, nonlinearity and amplitude can change the position and width of the band gap. This means that when the structure design is completed, the band gap can be changed by changing the amplitude, so that the elastic wave can be tuned.

This paper is organized as follows. In Section 2, we derive the dispersion expressions for one-dimensional linear and nonlinear elastic metamaterials. In Section 3, we discuss the tuning of different parameters on the amplitude-dependent band gap. Numerical simulations are presented in Section 4. The conclusions are drawn in Section 5.

2. Dispersion Relation of One-Dimensional Elastic Metamaterials

2.1. Linear Case

The model of the linear EMs is shown in Figure 1. The unit cells are connected by a spring with a stiffness of K_1 . In the unit cell, an oscillator with a mass of m is attached to a mass of M by a spring with a stiffness of K_2 . The distance between the two unit cells a is the so-called lattice constant.

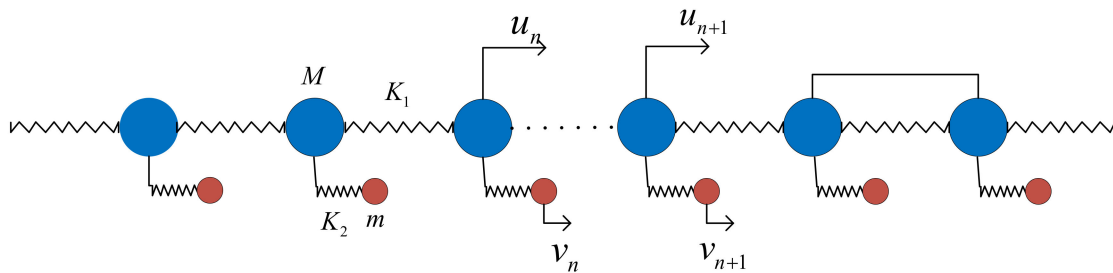


Figure 1. Linear one-dimensional mass-spring lattices attached with local resonators.

For the n -th unit cell, the motion equations of the mass and the attached oscillator can be written as:

$$M \frac{d^2 u_n}{dt^2} + K_1(2u_n - u_{n-1} - u_{n+1}) - K_2(v_n - u_n) = 0 \tag{1}$$

$$m \frac{d^2 v_n}{dt^2} + K_2(v_n - u_n) = 0 \tag{2}$$

where u_n is the displacement of the n -th mass on the main chain and v_n is the displacement of its additional local resonator, as shown in Figure 1. By introducing the coefficients $\omega_0 = \sqrt{\frac{K_1}{M}}$, $\alpha = \frac{m}{M}$ and $\beta = \frac{K_2}{K_1}$, Equations (1) and (2) can be written as:

$$\frac{d^2 u_n}{dt^2} + \omega_0^2(u_n - u_{n-1} - u_{n+1}) - \beta \omega_0^2(v_n - u_n) = 0 \tag{3}$$

$$\frac{d^2v_n}{dt^2} + \frac{\beta}{\alpha}\omega_0^2(v_n - u_n) = 0 \tag{4}$$

Based on Bloch’s theorem, the following equations can be obtained:

$$u_n = Ce^{i(\omega t - nka)} \tag{5}$$

$$v_n = De^{i(\omega t - nka)} \tag{6}$$

where C and D are the amplitudes of u_n and v_n , respectively, and k is the wave vector. By combining the equations above, the dispersion relation of the linear EMs can be obtained [41]:

$$\cos(ka) = 1 - \frac{(\frac{\beta}{\alpha} + \beta)\omega^2 - \frac{\omega^4}{\omega_0^2}}{2(\frac{\beta}{\alpha}\omega_0^2 - \omega^2)} \tag{7}$$

Normalized frequency $\bar{\omega} = \omega/\omega_1$ is introduced, where $\omega_1 = \sqrt{K_2/m}$. Then, Equation (7) can be simplified as:

$$\cos(ka) = 1 - (\frac{\beta}{2\alpha}\bar{\omega}^2 + \frac{\beta\bar{\omega}^2}{2(1 - \bar{\omega}^2)}) \tag{8}$$

For a given value of $\bar{\omega}$, if the real part of ka exists, the elastic wave can propagate in the structure. The range of $\bar{\omega}$ is the so-called passband and the rest is the band gap. The imaginary part of ka represents the attenuation characteristic of the band gap. Figure 2 shows the band gap of the linear elastic metamaterial at a mass ratio of $\alpha = 0.5$ and stiffness ratio of $\beta = 2$. It can be seen that the largest attenuation occurs at the natural frequency of the attached oscillator.

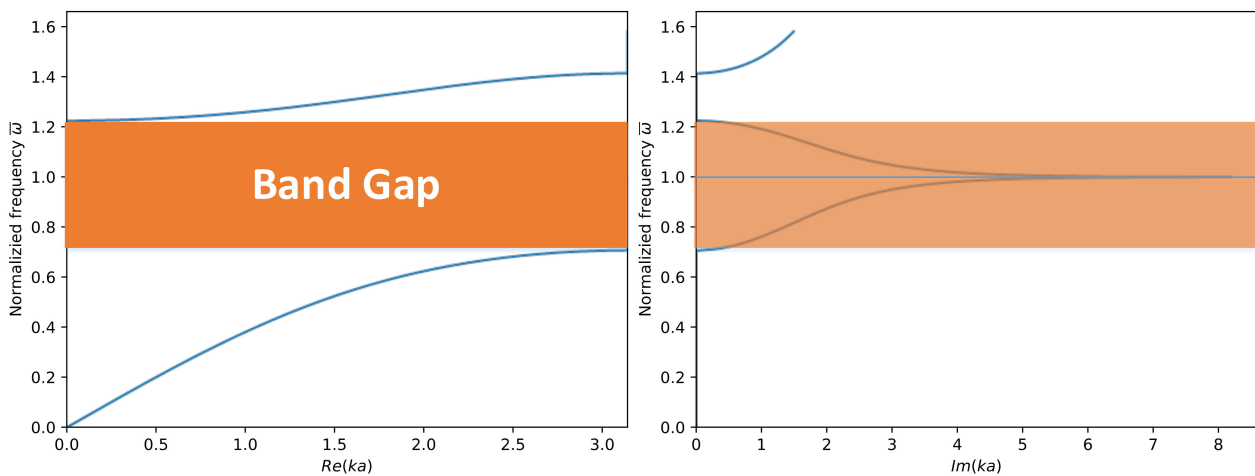


Figure 2. Dispersion curve of a one-dimensional linear elastic metamaterial with $\alpha = 0.5, \beta = 2$.

2.2. Nonlinear Case

In this section, we investigate the dispersion relation of the nonlinear EMs as shown in Figure 3. The unit cells are connected by a spring with a stiffness of K_1 . In the unit cell, an oscillator with a mass of m is attached to a mass of M by a nonlinear spring. The elastic force of the nonlinear spring is expressed as:

$$F = K_2x + \gamma K_2x^3 = K_2f(x) \tag{9}$$

where x is the deformation of the nonlinear spring, γ is a parameter controlling the degree of nonlinearity and $f(x) = x + \gamma x^3$. The motion equations of the n -th unit cell and the attached oscillator can be written as:

$$M\frac{d^2u_n}{dt^2} + K_1(2u_n - u_{n-1} - u_{n+1}) - K_2f((v_n - u_n)) = 0 \tag{10}$$

$$m \frac{d^2 v_n}{dt^2} + K_2 f((v_n - u_n)) = 0 \tag{11}$$

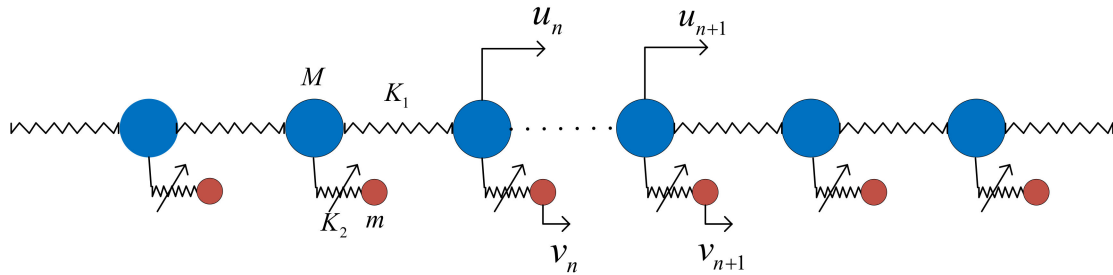


Figure 3. Nonlinear one-dimensional mass-spring lattices attached with local resonators.

By introducing $w_n = v_n - u_n$ and the parameters above Equation (3), the motion equations can be rewritten as:

$$\frac{d^2 u_n}{dt^2} + \omega_0^2 (u_n - u_{n-1} - u_{n+1}) - \beta \omega_0^2 f(w_n) = 0 \tag{12}$$

$$\frac{d^2 w_n}{dt^2} + \frac{\beta}{\alpha} \omega_0^2 f(w_n) + \frac{d^2 u_n}{dt^2} = 0 \tag{13}$$

Here, we adopt the harmonic balance method to solve the nonlinear equations. $w_n(t)$ is assumed to be complex Fourier series:

$$w_n(t) = \sum_j \varepsilon^{(j-1)/2} A_{j,n} e^{ij\omega t} + \varepsilon^{(j-1)/2} \bar{A}_{j,n} e^{-ij\omega t} \tag{14}$$

$j = 1, 3, 5 \dots$

where ε represents a small parameter. By substituting Equation (14) by Equation (13) and integrating twice with respect to time, the time response of mass n can be obtained as follows:

$$u_n(t) = A_{1,n} e^{i\omega t} \left(-1 + \frac{\beta}{\alpha \omega^2} + \frac{\gamma \beta}{\alpha \omega^2} \left(3A_{1,n} \bar{A}_{1,n} + \frac{3\varepsilon \bar{A}_{1,n}^2 A_{3,n}}{A_{1,n}} \right) \right) + \varepsilon A_{3,n} e^{3i\omega t} \left(-1 + \frac{\beta}{9\alpha \omega^2} + \frac{\beta \gamma}{9\alpha \omega^2} \left(\frac{A_{3,n}^3}{\varepsilon A_{3,n}} + 6A_{1,n} \bar{A}_{1,n} \right) \right) + c.c. + O(\varepsilon^2) \tag{15}$$

Based on Bloch’s theorem, the displacement of the mass n can be expressed as:

$$u_n(t) = \sum_j B_{n,j} e^{-inka} e^{ij\omega t} + c.c. \tag{16}$$

where $B_{n,j}$ is the coefficient in front of $e^{ij\omega t}$ in Equation (15). We assume the nonlinearities to be small, so the contributions to the solution of no less than third harmonics are neglected. Substituting Equations (14) and (16) by (12), equating the coefficient in front of $e^{ij\omega t}$ to zero, the dispersion relation for the nonlinear EMs is obtained as follows:

$$\cos(ka) = 1 - \frac{\bar{\omega}^2 \beta}{2\alpha} \left(1 + \frac{\alpha(1 + 3\gamma A_{1,n} \bar{A}_{1,n})}{1 + 3\gamma A_{1,n} \bar{A}_{1,n} - \bar{\omega}^2} \right) \tag{17}$$

It is evident that the dispersion relationship is affected by nonlinear parameters and amplitude. It is the same as the dispersion relation for the linear case in Equation (8), when the nonlinear parameter γ is equated to zero.

3. Tuning on the Nonlinear Band Gap

In Equations (8) and (14), let $\cos(ka) = 1$ or -1 , and the starting and ending frequencies of the band gap can be obtained, respectively. For the linear case:

$$\omega_{l-start} = \sqrt{\frac{(1 + \alpha + \frac{4\alpha}{\beta}) - \sqrt{(1 + \alpha + \frac{4\alpha}{\beta})^2 - \frac{16\alpha}{\beta}}}{2}} \tag{18}$$

$$\omega_{l-end} = \sqrt{1 + \alpha} \tag{19}$$

In the nonlinear case:

$$\omega_{n-start} = \sqrt{\frac{c - \sqrt{c^2 - 16\beta(\alpha + 3\alpha\gamma A_{1,n}\bar{A}_{1,n})}}{2\beta}} \tag{20}$$

$$\omega_{n-end} = \sqrt{(1 + \alpha)(1 + 3\gamma A_{1,n}\bar{A}_{1,n})} \tag{21}$$

where $c = 4\alpha + \beta + \alpha\beta + 3\beta\gamma A_{1,n}\bar{A}_{1,n} + 3\alpha\beta\gamma A_{1,n}\bar{A}_{1,n}$.

Figure 4 shows the effect of mass ratio on the band gap of the linear EMs and Figure 5 shows the nonlinear case. It shows that both the ending and starting frequencies of the stopband increase with the increase in the attached mass, regardless of whether it is linear or nonlinear. Additionally, the width of the band gap also increases. A more detailed comparison is shown in Figure 6. For the nonlinear EMs, the ending frequency of the band gap is about 26% higher than that of the linear EMs, while the starting frequency is slightly increased. This indicates that nonlinearity can significantly enhance the influence of the mass ratio on the band gap.

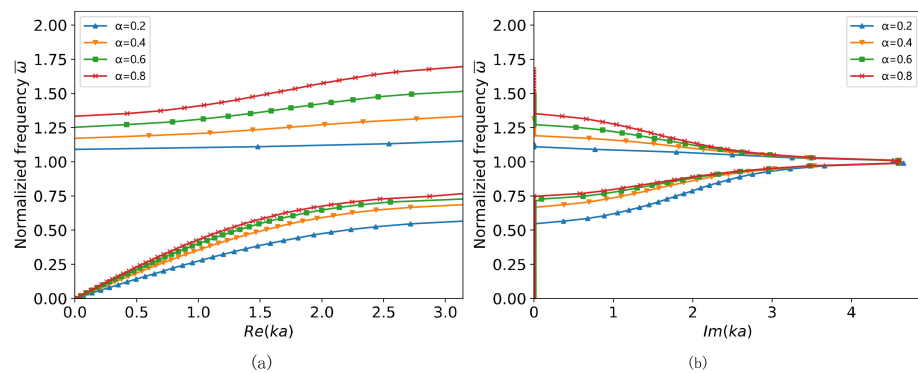


Figure 4. Dispersion relation for the linear EMs with $\beta = 2$ and different mass ratio.

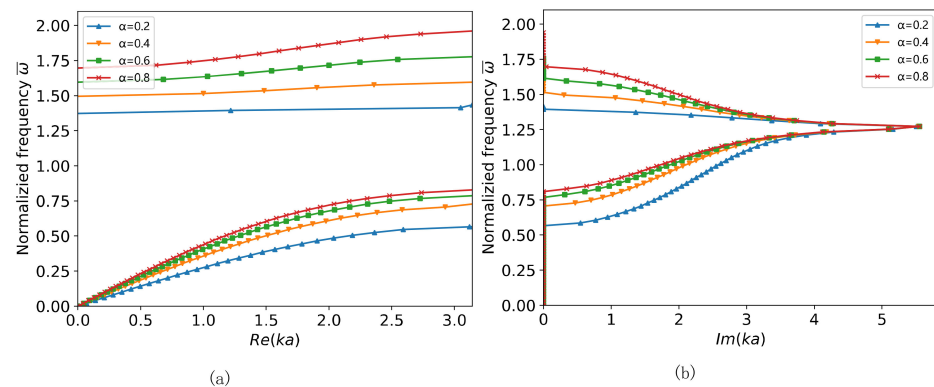


Figure 5. Dispersion relation for the nonlinear Ems with $\beta = 2, \gamma A_{1,n}\bar{A}_{1,n} = 0.2$ and different mass ratio.

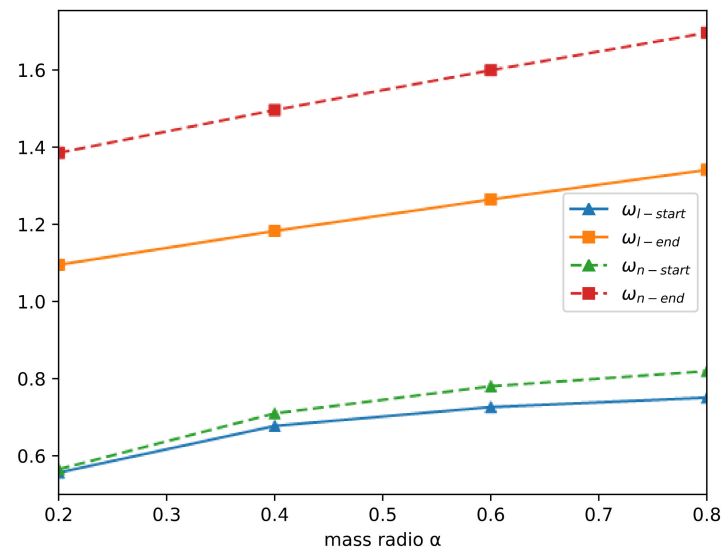


Figure 6. Effect of mass ratio on starting and ending frequency.

Figures 7 and 8 show the effect of stiffness ratio β on the band gap in the linear and nonlinear EMs, respectively. Figure 9 shows the trends of the starting and ending frequencies with respect to the stiffness ratio. The greater the ratio of linear stiffness ratio β is, the greater the band gap is. Different from the mass ratio, the change of stiffness ratio almost does not affect the ending frequency of the band gap, but it will make the starting frequency smaller. Compared with the linear EMs, both the starting and ending frequencies of the nonlinear case are increased, but the width of the band gap is not significantly increased.

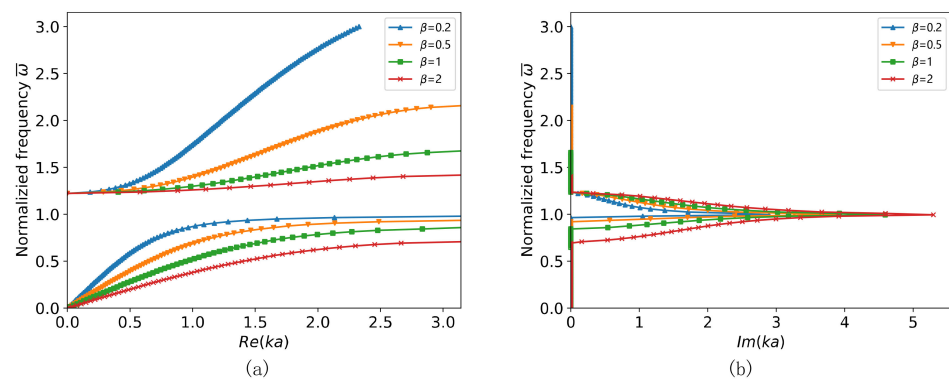


Figure 7. Dispersion relation for the linear EMs with $\alpha = 0.5$ and different β .

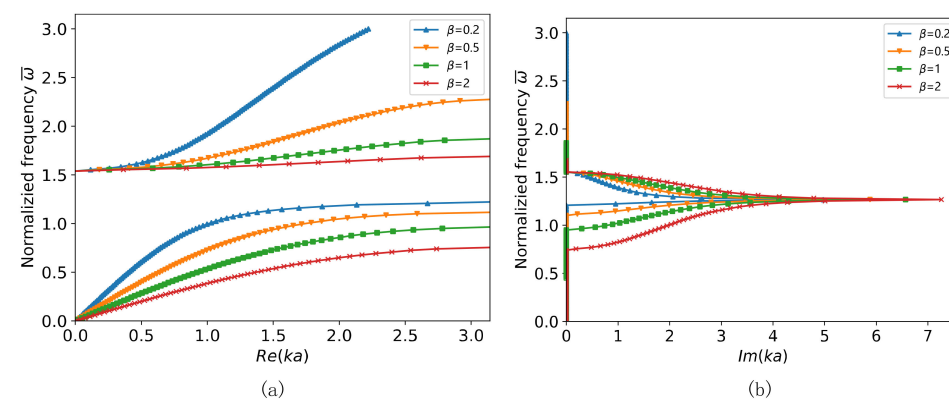


Figure 8. Dispersion relation for the nonlinear EMs with $\alpha = 0.5$, $\gamma A_{1,n} \bar{A}_{1,n} = 0.2$ and different β .

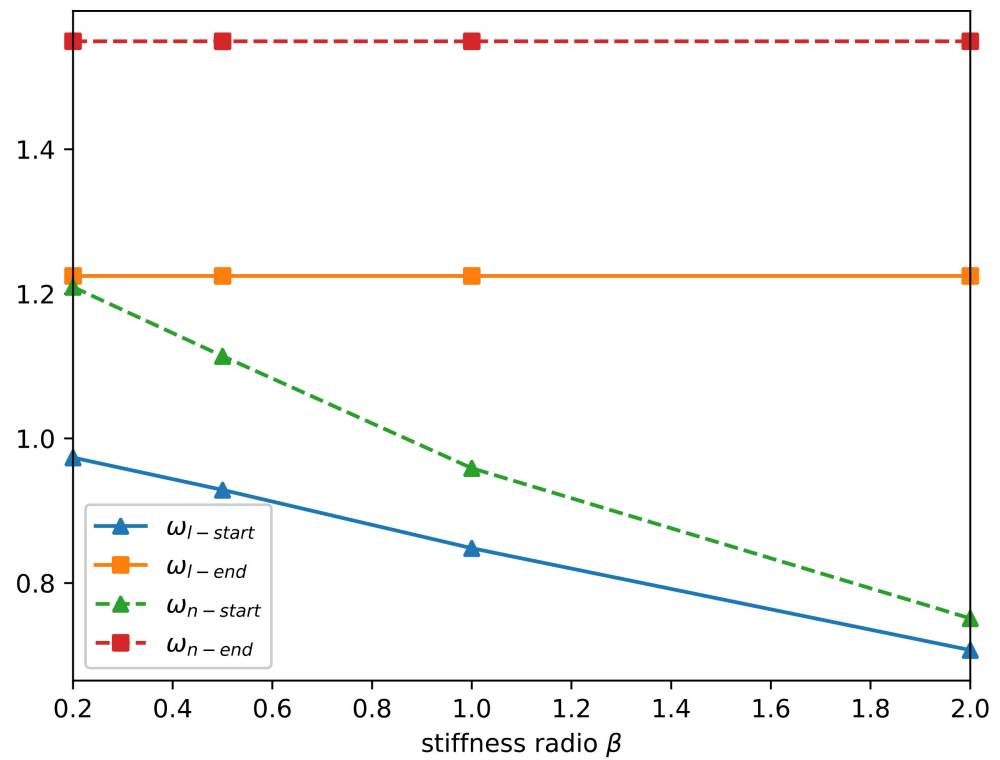


Figure 9. Effect of stiffness ratio on starting and ending frequencies.

Figure 10 shows the effect of nonlinear parameter $\gamma A_{1,n} \bar{A}_{1,n}$ on the stopband in the EMs. Figure 11 shows the trends of the starting and ending frequencies with the change in the nonlinear parameter. It can be seen that when the nonlinear parameters increase, the ending frequency of the band gap increases greatly, while the starting frequency increases marginally. As a result, the width of the band gap increases significantly. In addition, the position of the maximum value of the attenuation is shifted above the linear natural frequency.

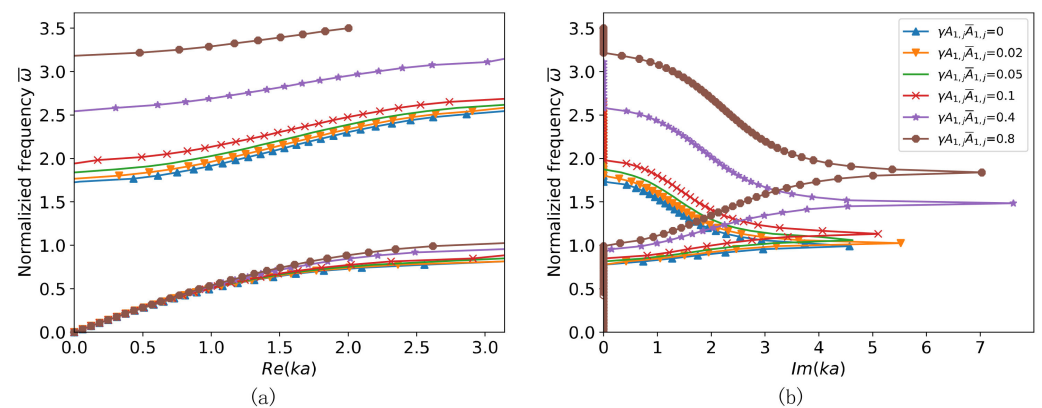


Figure 10. Dispersion relation for the linear EMs with $\alpha = 0.5$, $\beta = 2$ and different $\gamma A_{1,n} \bar{A}_{1,n}$.

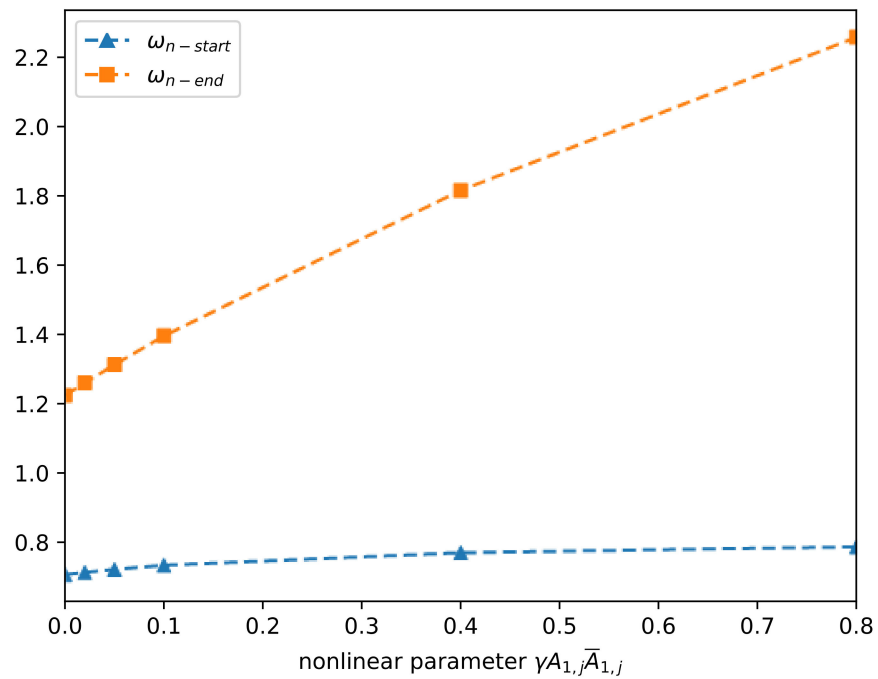


Figure 11. Effect of nonlinear parameter on starting and ending frequencies.

4. Numerical Simulation

The above solution of the vibration band gap of the one-dimensional mass-spring chain is carried out under the infinite period structure. In this section, the numerical calculation method is adopted to calculate the vibration transmission properties of the mass-spring structure with finite period. A diagram of the finite structure is shown in Figure 12. The transmission properties of the finite lattices are defined as follows:

$$tr = 20 \log_{10} \left| \frac{u_{out}}{u_{in}} \right| \tag{22}$$

where u_{out} is the response of the output point and u_{in} is the amplitude of the input point. Here, we apply sine sweep displacement excitation, with a frequency band from 1 to 20 Hz and an amplitude U to the first unit cell and measure the response at the n -th cell. Specific parameters are shown in Table 1.

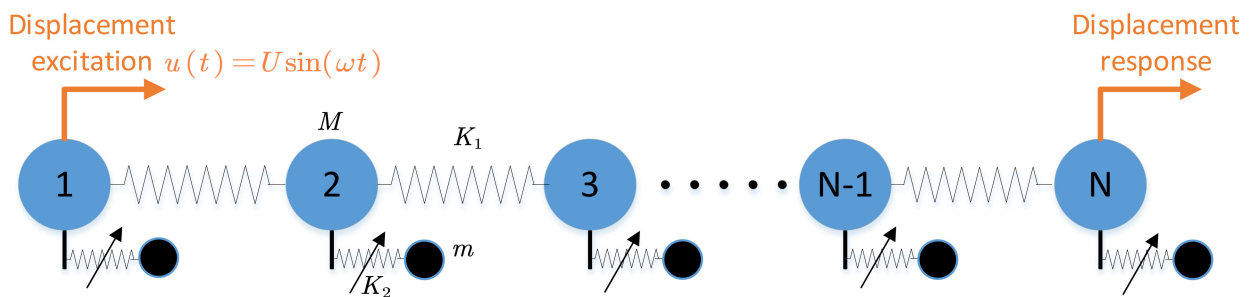


Figure 12. Schematics of a finite 1D mass-spring chain with attached local resonators.

Table 1. Parameters of finite lattices.

K_1	K_2	M	m
1000 N/m	2000 N/m	1 kg	0.5 kg

Figures 13–15 show the effects of unit cell number, amplitude of the displacement excitation and nonlinearity on the transmission properties of the mass-spring chain attached with nonlinear local resonators. Figure 13 shows that the increase in the cell number does not change the band gap width, but the vibration attenuation in the band gap range becomes increasingly larger. Figures 14 and 15 show that the increase in excitation amplitude and nonlinearity have little effect on the lower boundary of the band gap, but will increase the upper boundary. This indicates a good agreement with the theoretical analysis in Section 3. However, in the numerical simulation, the influence of amplitude and nonlinearity on the upper boundary of the band gap is not as great as that in the theoretical analysis. This mainly takes into account the fact that the amplitude in Section 3 is not consistent with the amplitude of displacement excitation. Although the simulation method has disadvantages, the trend of the band gap change caused by nonlinearity and amplitude still coincides with the analytical results.

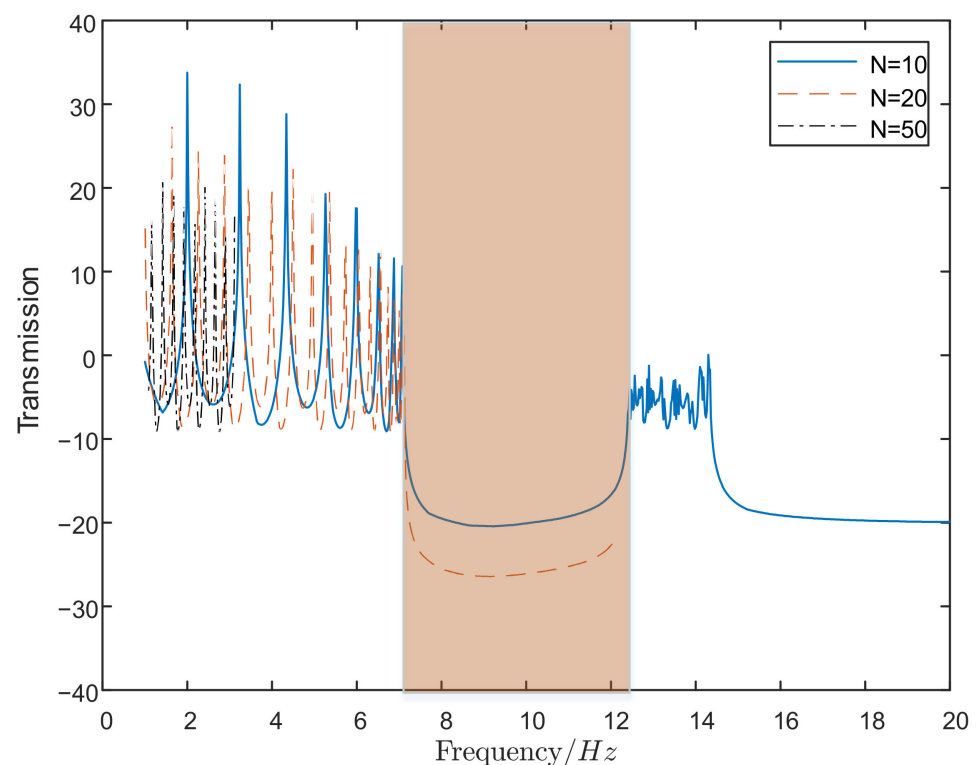


Figure 13. Influence of unit cell number on band gap ($U = 0.1; \gamma = 0.05$).

We also choose two typical frequencies, $f = 4$ Hz and $f = 10$ Hz, to represent the corresponding responses in the passband and band gap, respectively. Figures 16 and 17 are time domain and frequency domain diagrams of excitation and response at $f = 4$ Hz, respectively. Figures 18 and 19 are the case at $f = 10$ Hz. It can be clearly seen that the elastic wave can propagate without attenuation in the passband, while it delays significantly in the band gap.

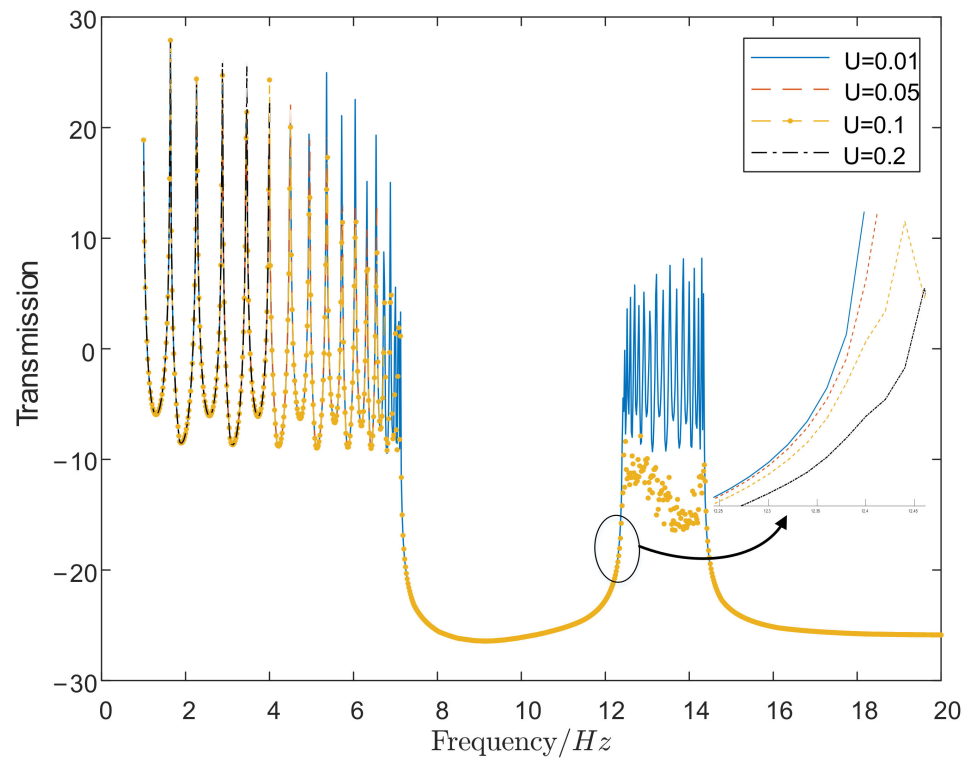


Figure 14. Influence of displacement excitation amplitude on band gap ($\gamma = 0.2; N = 20$).

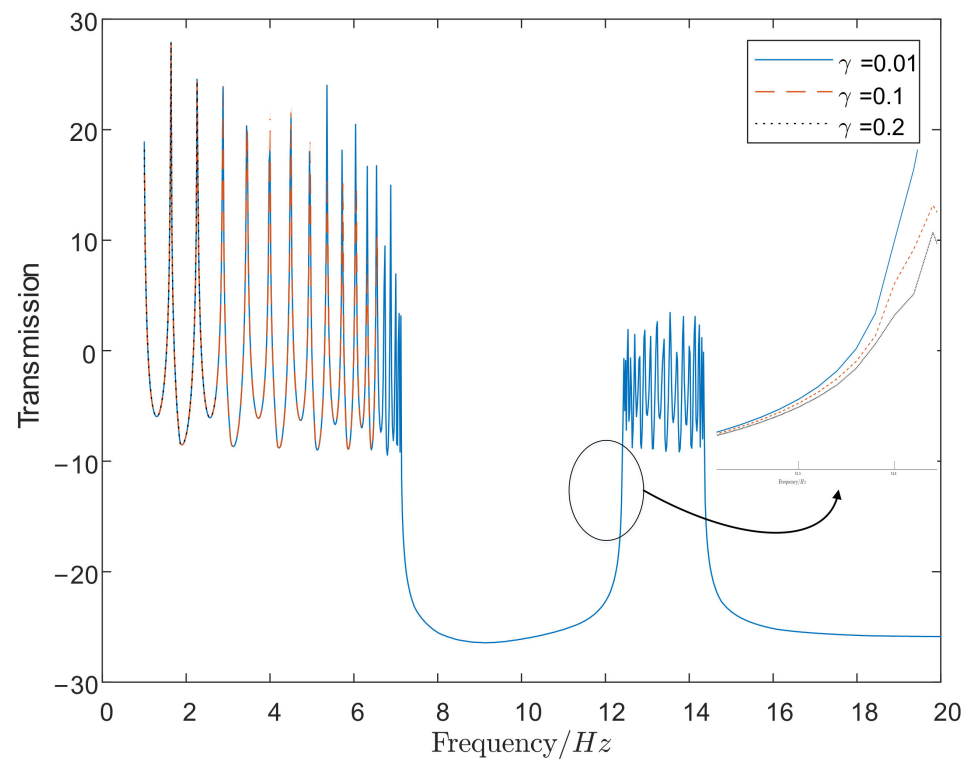


Figure 15. Influence of nonlinearity on band gap ($U = 0.1; N = 20$).

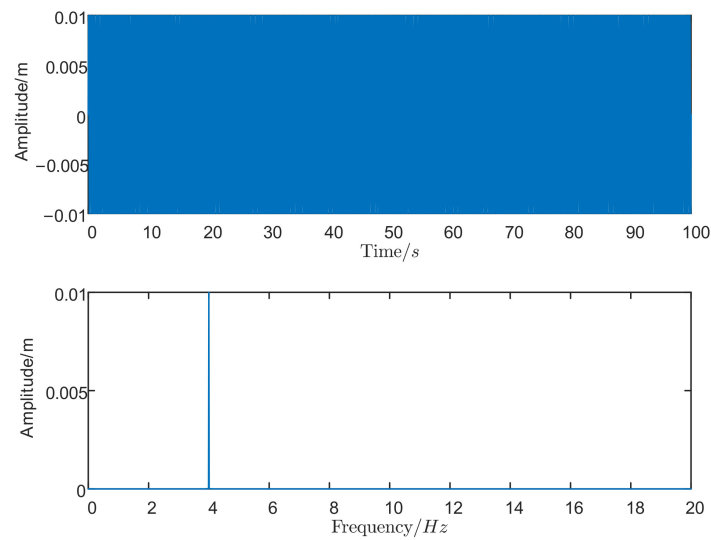


Figure 16. Time histories and FFT result of displacement excitation at $f = 4$ Hz.

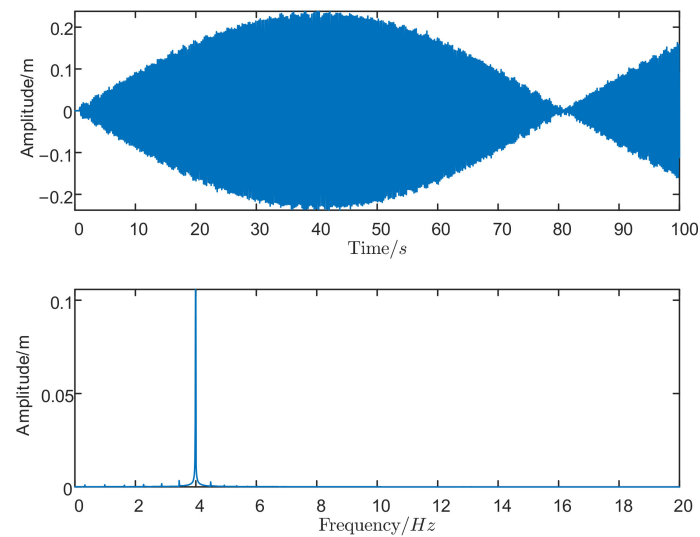


Figure 17. Time histories and FFT result of displacement response.

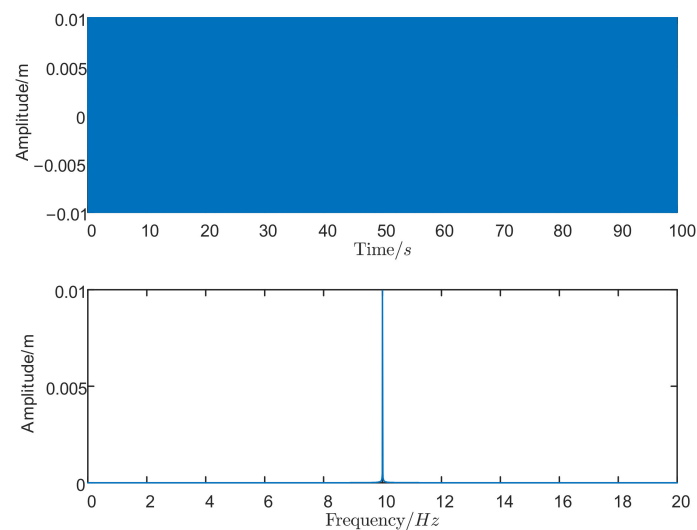


Figure 18. Time histories and FFT result of displacement excitation at $f = 10$ Hz.

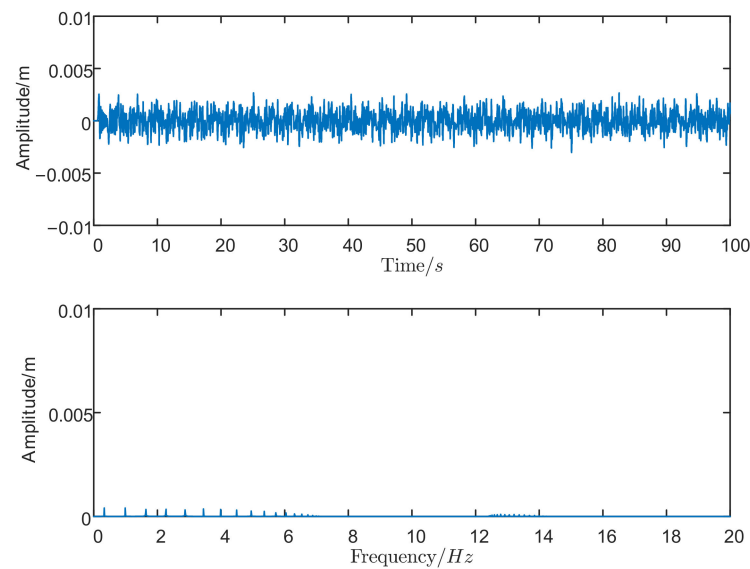


Figure 19. Time histories and FFT result of displacement response.

5. Conclusions

In this paper, we focus on the nonlinear tunability of elastic waves in one-dimensional mass-spring lattices attached with local resonators. The harmonic balance method is applied to derive the nonlinear dispersion relation and a concise expression of wave vector and normalized frequency is obtained. The results show that the band gap can be adjusted by mass ratio, stiffness ratio, nonlinearity and displacement amplitude. The mass ratio can increase both the upper and lower boundary of the band gap. However, it has little effect on the width of the band gap. The linear stiffness ratio has little effect on the upper boundary of the band gap, but the lower boundary decreases significantly with the increase in the stiffness ratio. This means that the width of the band gap increases. By changing the nonlinearity or displacement amplitude, the band gap can be shifted and the width of the band gap visibly increases. With the increase in nonlinear parameters, the maximum value of attenuation shifts above the linear natural frequency of local resonators. Then, a numerical simulation is carried out to obtain the transmission properties of the finite mass-spring lattices attached with local resonators. The result shows that the analytical predictions are in good agreement with the simulations. Our research discusses the tuning effect of various parameters on elastic waves in nonlinear EMs in detail, which provides a potential application for vibration reduction.

Author Contributions: Conceptualization, J.J. and F.Z.; methodology and formal analysis, N.S.; validation and supervision, J.J. and F.Z.; investigation, J.J. and N.S.; writing—original draft preparation, N.S.; writing—review and editing, N.S. and M.D. All authors have read and agreed to the published version of the manuscript.

Funding: Our research is supported by the Foundation of National Key Laboratory of Science and Technology on Rotorcraft Aeromechanics (No. 61422202105) and the Qing Lan Project.

Institutional Review Board Statement: Not applicable.

Informed Consent Statement: Not applicable.

Data Availability Statement: All data included in this study are available upon request by contact with the corresponding author.

Conflicts of Interest: The authors declare no conflict of interest.

References

1. He, C.; Zhang, F.; Jiang, J. Adaptive Boundary Control of Flexible Manipulators with Parameter Uncertainty Based on RBF Neural Network. *Shock Vib.* **2020**, *2020*, 8261423. [[CrossRef](#)]

2. Ibrahim, R. Recent advances in nonlinear passive vibration isolators. *J. Sound Vib.* **2008**, *314*, 371–452. [[CrossRef](#)]
3. Baravelli, E.; Ruzzene, M. Internally resonating lattices for bandgap generation and low-frequency vibration control. *J. Sound Vib.* **2013**, *332*, 6562–6579. [[CrossRef](#)]
4. Madeo, A.; Collet, M.; Miniaci, M.; Billon, K.; Ouisse, M.; Neff, P. Modeling Phononic Crystals via the Weighted Relaxed Micromorphic Model with Free and Gradient Micro-Inertia. *J. Elast.* **2018**, *130*, 59–83. [[CrossRef](#)]
5. Witarto, W.; Nakshatrala, K.B.; Mo, Y.-L. Global sensitivity analysis of frequency band gaps in one-dimensional phononic crystals. *Mech. Mater.* **2019**, *134*, 38–53. [[CrossRef](#)]
6. Mo, C.; Singh, J.; Raney, J.R.; Purohit, P.K. Cnoidal wave propagation in an elastic metamaterial. *Phys. Rev. E* **2019**, *100*, 013001. [[CrossRef](#)] [[PubMed](#)]
7. Liu, Z.; Zhang, X.; Mao, Y.; Zhu, Y.Y.; Yang, Z.; Chan, C.T.; Sheng, P. Locally Resonant Sonic Materials. *Science* **2000**, *289*, 1734–1736. [[CrossRef](#)] [[PubMed](#)]
8. Ma, G.; Sheng, P. Acoustic metamaterials: From local resonances to broad horizons. *Sci. Adv.* **2016**, *2*, e1501595. [[CrossRef](#)]
9. Liu, J.; Guo, H.; Wang, T. A Review of Acoustic Metamaterials and Phononic Crystals. *Crystals* **2020**, *10*, 305. [[CrossRef](#)]
10. Kumar, S.; Lee, H. Recent Advances in Acoustic Metamaterials for Simultaneous Sound Attenuation and Air Ventilation Performances. *Crystals* **2020**, *10*, 686. [[CrossRef](#)]
11. Choi, C.; Bansal, S.; Münzenrieder, N.; Subramanian, S. Fabricating and Assembling Acoustic Metamaterials and Phononic Crystals. *Adv. Eng. Mater.* **2021**, *23*, 2000988. [[CrossRef](#)]
12. He, C.; Lim, K.-M.; Zhang, F.; Jiang, J.-H. Dual-tuning mechanism for elastic wave transmission in a triatomic lattice with string stiffening. *Wave Motion Int. J. Report. Res. Wave Phenom.* **2022**, *112*, 102951. [[CrossRef](#)]
13. He, C.; Lim, K.M.; Liang, X.; Zhang, F.; Jiang, J. Tunable band structures design for elastic wave transmission in tension metamaterial chain. *Eur. J. Mech. A/Solids* **2022**, *92*, 104481. [[CrossRef](#)]
14. Liang, X.; Zhang, F.; Jiang, J. Ultra-wideband outward-hierarchical metamaterials with graded design. *Int. J. Mech. Mater. Des.* **2022**, *18*, 169–184. [[CrossRef](#)]
15. Wang, Y.-F.; Wang, T.-T.; Liang, J.-W.; Wang, Y.-S.; Laude, V. Channeled spectrum in the transmission of phononic crystal waveguides. *J. Sound Vib.* **2018**, *437*, 410–421. [[CrossRef](#)]
16. Chen, Z.-G.; Zhao, J.; Mei, J.; Wu, Y. Acoustic frequency filter based on anisotropic topological phononic crystals. *Sci. Rep.* **2017**, *7*, 15005. [[CrossRef](#)]
17. Zigoneanu, L.; Popa, B.-I.; Cummer, S.A. Three-dimensional broadband omnidirectional acoustic ground cloak. *Nat. Mater.* **2014**, *13*, 352–355. [[CrossRef](#)]
18. Casadei, F.; Beck, B.S.; Cunefare, K.A.; Ruzzene, M. Vibration control of plates through hybrid configurations of periodic piezoelectric shunts. *J. Intell. Mater. Syst. Struct.* **2012**, *23*, 1169–1177. [[CrossRef](#)]
19. Wu, X.; Sun, L.; Zuo, S.; Liu, P.; Huang, H. Vibration reduction of car body based on 2D dual-base locally resonant phononic crystal. *Appl. Acoust.* **2019**, *151*, 1–9. [[CrossRef](#)]
20. Brooke, D.C.; Umnova, O.; Leclaire, P.; Dupont, T. Acoustic metamaterial for low frequency sound absorption in linear and nonlinear regimes. *J. Sound Vib.* **2020**, *485*, 115585. [[CrossRef](#)]
21. Chen, J.; Xiao, J.; Lisevych, D.; Shakouri, A.; Fan, Z. Deep-subwavelength control of acoustic waves in an ultra-compact metasurface lens. *Nat. Commun.* **2018**, *9*, 4920. [[CrossRef](#)] [[PubMed](#)]
22. Kaina, N.; Lemoult, F.; Fink, M.; Lerosey, G. Negative refractive index and acoustic superlens from multiple scattering in single negative metamaterials. *Nature* **2015**, *525*, 77–81. [[CrossRef](#)] [[PubMed](#)]
23. Miniaci, M.; Gliozzi, A.S.; Morvan, B.; Krushynska, A.; Bosia, F.; Scalerandi, M.; Pugno, N.M. Proof of Concept for an Ultrasensitive Technique to Detect and Localize Sources of Elastic Nonlinearity Using Phononic Crystals. *Phys. Rev. Lett.* **2017**, *118*, 214301. [[CrossRef](#)] [[PubMed](#)]
24. Li, Z.-N.; Wang, Y.-Z.; Wang, Y.-S. Nonreciprocal phenomenon in nonlinear elastic wave metamaterials with continuous properties. *Int. J. Solids Struct.* **2018**, *150*, 125–134. [[CrossRef](#)]
25. Wang, Y.-Z.; Li, F.-M.; Kishimoto, K. Effects of the initial stress on the propagation and localization properties of Rayleigh waves in randomly disordered layered piezoelectric phononic crystals. *Acta Mech.* **2011**, *216*, 291–300. [[CrossRef](#)]
26. Kherraz, N.; Haumesser, L.; Levassort, F.; Benard, P.; Morvan, B. Controlling Bragg gaps induced by electric boundary conditions in phononic piezoelectric plates. *Appl. Phys. Lett.* **2016**, *108*, 093503. [[CrossRef](#)]
27. Li, G.-H.; Ma, T.-X.; Wang, Y.-Z.; Wang, Y.-S. Active control on topological immunity of elastic wave metamaterials. *Sci. Rep.* **2020**, *10*, 9376. [[CrossRef](#)]
28. Wu, Y.; Yu, K.; Yang, L.; Zhao, R.; Shi, X.; Tian, K. Effect of thermal stresses on frequency band structures of elastic metamaterial plates. *J. Sound Vib.* **2018**, *413*, 101–119. [[CrossRef](#)]
29. Bordiga, G.; Cabras, L.; Piccolroaz, A.; Bigoni, D. Prestress tuning of negative refraction and wave channeling from flexural sources. *Appl. Phys. Lett.* **2019**, *114*, 041901. [[CrossRef](#)]
30. Xu, X.; Wu, Q.; Chen, H.; Nassar, H.; Chen, Y.; Norris, A.; Haberman, M.R.; Huang, G. Physical Observation of a Robust Acoustic Pumping in Waveguides with Dynamic Boundary. *Phys. Rev. Lett.* **2020**, *125*, 253901. [[CrossRef](#)]
31. Banerjee, A.; Das, R.; Calius, E.P. Waves in Structured Mediums or Metamaterials: A Review. *Arch. Comput. Methods Eng.* **2018**, *26*, 1029–1058. [[CrossRef](#)]

32. Fang, X.; Wen, J.; Yu, D.; Huang, G.; Yin, J. Wave propagation in a nonlinear acoustic metamaterial beam considering third harmonic generation. *New J. Phys.* **2018**, *20*, 123028. [[CrossRef](#)]
33. Yu, M.; Fang, X.; Yu, D. Combinational design of linear and nonlinear elastic metamaterials. *Int. J. Mech. Sci.* **2021**, *199*, 106422. [[CrossRef](#)]
34. Bae, M.H.; Oh, J.H. Amplitude-induced bandgap: New type of bandgap for nonlinear elastic metamaterials. *J. Mech. Phys. Solid* **2020**, *139*, 103930. [[CrossRef](#)]
35. Fang, X.; Wen, J.; Bonello, B.; Yin, J.; Yu, D. Ultra-low and ultra-broad-band nonlinear acoustic metamaterials. *Nat. Commun.* **2017**, *8*, 1288. [[CrossRef](#)] [[PubMed](#)]
36. Fang, X.; Wen, J.; Bonello, B.; Yin, J.; Yu, D. Wave propagation in one-dimensional nonlinear acoustic metamaterials. *New J. Phys.* **2017**, *19*, 53007. [[CrossRef](#)]
37. Vakakis, A.F.; King, M.E. Nonlinear wave transmission in a monocoupled elastic periodic system. *J. Acoust. Soc. Am.* **1995**, *98*, 1534–1546. [[CrossRef](#)]
38. Silva, P.B.; Leamy, M.J.; Geers, M.G.D.; Kouznetsova, V.G. Emergent subharmonic band gaps in nonlinear locally resonant metamaterials induced by autoparametric resonance. *Phys. Rev. E* **2019**, *99*, 063003. [[CrossRef](#)]
39. Manktelow, K.L.; Leamy, M.J.; Ruzzene, M. Weakly nonlinear wave interactions in multi-degree of freedom periodic structures. *Wave Motion* **2014**, *51*, 886–904. [[CrossRef](#)]
40. Wei, L.-S.; Wang, Y.-Z.; Wang, Y.-S. Nonreciprocal transmission of nonlinear elastic wave metamaterials by incremental harmonic balance method. *Int. J. Mech. Sci.* **2020**, *173*, 105433. [[CrossRef](#)]
41. Huang, H.H.; Sun, C.T.; Huang, G.L. On the negative effective mass density in acoustic metamaterials. *Int. J. Eng. Sci.* **2009**, *47*, 610–617. [[CrossRef](#)]